Essential Readings in Light Metals: Aluminum Reduction Technology.
Edited by Geoff Bearne, Marc Dupuis and Gary Tarcy.

ON THE BATH FLOW, ALUMINA DISTRIBUTION AND ANODE GAS RELEASE IN ALUMINIUM CELLS

Ove Kobbeltvedt * and Bjørn P. Moxnes**

* SINTEF Materials Technology, N-7034 Trondheim, Norway
** Hydro Aluminium, Technology Centre Årdal,
N-5870 Øvre Årdal, Norway

Abstract

The bath flow was studied in prebake cells. The measurements were performed by recording the drop in bath temperature subsequent to alumina feeding as well as by adding tracer to the bath followed by subsequent bath sampling. The horizontal flow rate varied between 2 and 10 cm/s. It was found that the horizontal bath flow in the bulk above the working surface of the anodes and consequently the alumina distribution pattern are mainly determined by the bath flow from underneath the anodes. The quantity of anode gas which was drained into the centre channel was measured at different locations in a cell. The results showed that the distribution of the anode gas in the bath is strongly associated with the bath flow pattern under the anodes.

Introduction

In aluminium production it is essential to be able to run the reduction cells at the optimum level. One of the most important factors in the efforts to achieve optimum cell operation is the mixing of alumina in the bath phase. The objective is to keep the alumina concentration at a uniform level throughout the bath volume with as little variation as possible. With modern point feeding the alumina is added into a limited part of the bath volume. Accumulation of alumina in the vicinity of the feeder can lead to sludge formation. Therefore, effective distribution of the alumina from the feeding point is important to prevent mucky cells. On the other hand, if the bath flow is directed into certain parts of the cell, permanent gradients in alumina concentration in the bath can be the result. For optimum cell performance all the alumina added should be distributed evenly *as dissolved species* into the anode-cathode gap (ACG).

Studies of bath flow in the literature

The distribution of alumina in the bath phase is dependent upon the bath flow. Magnetohydrodynamic (MHD) forces, drag forces between escaping anode gas and bath as well as thermal gradients create convection in the bath phase. When comparing these three factors the latter is usually considered to be the least important for the overall bath flow.

Most work in this field has been done on mathematical and physical modelling. In both the mathematical and physical modelling reported in the literature, important assumptions were usually made. With some exceptions, either only the gas driven flow or only the MHD induced flow has been considered.

Physical modelling using aqueous systems where only gas driven flow has been considered, is widely reported in the literature [1-7]. In one study, however, [8] physical modelling work was performed where only the MHD-forces were considered. In that case Wood's metal was used to simulate the electrolyte.

The studies that have been made with computer modelling are mostly restricted to MHD-driven flow only [9-11]. Bilek et al. [12] combined the effects of MHD and gas driven forces in a modelling work where the computer program FLUENT was used. From this work it was concluded that gas release dominates the electrolyte flow field.

Bath flow measurements in real systems are scarce, probably due to the difficulties involved in measuring bath flow in cryolitic melts. Grjotheim et al. [13] measured bath flow as well as metal flow in reduction cells with the use of radioactive tracers. They found that the vertical velocity gradients were small through a liquid cell volume. Furthermore, they observed a rather unstable flow situation in the bath.

In the present work bath flow was measured in reduction cells. The motivation for the measurement program was the problems concerning alumina distribution in the bath. Most of the results presented in this paper were achieved by monitoring the temperature depression which follows an alumina addition to the bath. In some cases tracer (NaCl) was added through the feeding holes followed by frequent bath sampling.

The amount of anode gas released from the short sides of anodes in a side-by-side cell was also measured. This was done by collecting the gas in a funnel placed at different locations at the short sides of the anodes.

Background:

One of the incentives for the measurements described in this paper was the experience gained by the operating personnel regarding at which positions in the cell anode problems were most likely to occur. The cells were in side-by-side configuration and problems here mean initiation of spikes and deformations on the working surface of the anodes. The occurrence of spikes and deformations is usually detected by increased noise in the recorded cell resistance. The procedure is

then to remove the anode from the cell and level the underside in a special milling machine. It is well known from cell operation that anode problems are more likely to occur with acid baths and low bath temperatures. Furthermore, statistics on the frequency of anode problems are significantly correlated with anode location.

Fig. 1 shows a section of the cell in the present study, while Figs. 2 and 3 shows bar charts for the proportion of the total number of deformation as a function of anode position on the upstream and downstream sides respectively. The statistics are based on all anode deformations which were recorded in a two months period.

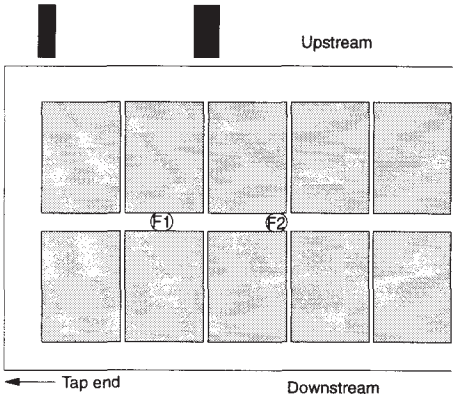

Figure 1 - A section of the cell in the present study showing the positions of two of the feeders (labelled "F1" and "F2") and the positions of the risers.

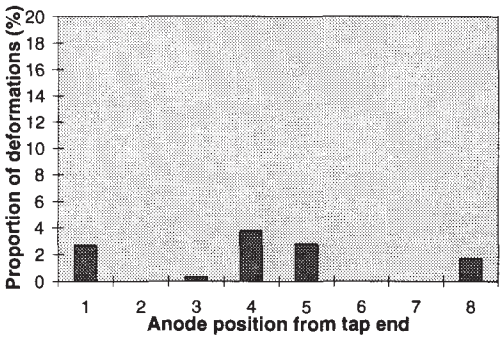

Figure 2 - The proportion of the total number of deformation on the anodes on the upstream side in the cell shown in Fig. 1.

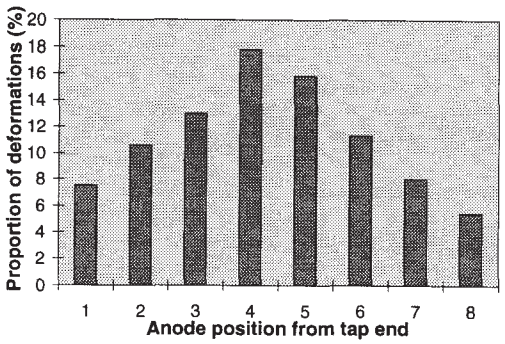

Figure 3 - The proportion of the total number of deformation on the anodes on the downstream side in the cell shown in Fig. 1.

The frequency of spike formation on the working surface of the anode underside as a function of location is analogous to the deformation statistics. As can be seen from Figs. 2 and 3, the frequency of deformations is clearly higher on the downstream side. Furthermore, the anodes located on the mid-section of the downstream side are particularly vulnerable to these problems, while the anodes on the upstream side near the quarter risers are practically immune to deformations as well as spikes.

Prior to this study bath samples were collected in two positions in the cell. The bath sampling was performed in the vicinity of anodes 4 and 5 counted from the tap end on the downstream side and in the vicinity of anodes 2 and 3 on the upstream side. As can be seen from the anode deformation statistics, these positions were selected based on where in the cell anode problems were the most and least likely to occur. Analysis of bath samples did show that the alumina concentration was significantly lower in the former position compared to the latter position. This situation proved to be permanent and thus not dependent upon the feeding cycle. Prior to this study it had therefore been concluded that the pattern of anode problems is correlated with a permanent gradient with respect to alumina in the bath on these cells.

The objective for the bath flow measurements in the present study was to clarify the alumina distribution pattern in the cells under study and hopefully to be able to explain some of the mechanisms behind it.

Experimental

Tracer addition

In order to get a first view of the bath flow pattern tracer additions were made to the bath through the feeding holes. Two kg NaCl was added followed by frequent bath sampling in selected locations in the cell. The sampling was simply performed by dipping an iron rod into the bath, immediately pulling it out, knocking off the frozen bath. The bath samples were taken in the gaps between the anodes traverse to the centre channel except for the position at the short end of the cell where the bath samples were collected in the tap hole. An assortment of the bath samples was later analysed (XRF) with respect to chloride.

Temperature measurements

The method that was applied in the main part of this study was continuous monitoring of the temperature depression which follows an alumina addition to the bath. This was achieved by placing several thermocouples in different locations in the bath and connecting them to a logging device.

The thermocouples, which were of the type K, were immersed vertically into the bath, the lower end located between the working surface of the anodes and the bath surface. The depth of immersion of the thermocouples was approximately 8 cm beneath the bath surface. The thermocouples were protected from the corrosive cryolitic melt by a steel tube with a wall thickness of 1 mm. The temperature of each thermocouple was logged every second by one or two *Campbell Scientific 21X Microloggers*. Prior to one logging period one of the feeders was set to a constant feeding rate (one batch every 90 to 100 s) while the other feeders were turned off. The duration of one logging period was 18-20 minutes.

The mean horizontal bath velocity between the feeder and a thermocouple could easily be estimated by dividing the distance between the feeding point and the nearest thermocouple by the time delay between feeding and the onset of a temperature drop in the thermocouple. Similarly the mean velocity between two thermocouples could be estimated from the times for the recorded temperature drop in each of the thermocouples.

In one case a thermocouple was placed in the ACG. The tip of the thermocouple was positioned into the ACG through a hole in the anode. The hole was drilled from the top of the anode down to 2-3 cm above the underside. One and a half to two days after the anode was set, the rest of the hole was opened with the aid of an iron rod, and the thermocouple was lowered into the hole where it quickly got stuck by the bath flowing into the hole and freezing.

Anode gas collection

The amount of gas released on the short sides of the anodes was measured by recording the time needed for the anode gas collected through a funnel to displace 1.55 litre of silicon oil. The funnel, which was 15 cm wide, was pressed on to the short side of the anode.

Before starting the measurement the anode was removed from the cell for removal of adhering bath. One hour after resetting the current through the anode was measured. The measurement was started when the current through the anode was back to normal.

Results

In the following results are given from six measuring campaigns. In campaign I tracer additions with subsequent bath sampling were performed. In campaigns II to V temperature measurements were performed. Finally, campaign VI was devoted to anode gas collection. All the campaigns with temperature recording were performed on the same cell.

The results on bath flow are given from measurements on the half of the cell which was near the tap end. Measurements carried out on the other side of the cell led to the same conclusions.

The feeders labelled "F1" and "F2" in Fig. 1 are in the following referred to as the outer and inner feeder, respectively.

Alumina transferred from an outer feeder

Fig. 4 shows the positions where the bath samples were collected after adding tracer to feeding position F1, while Figs. 5 and 6 show the relative chloride concentration in the four positions as a function of time after addition.

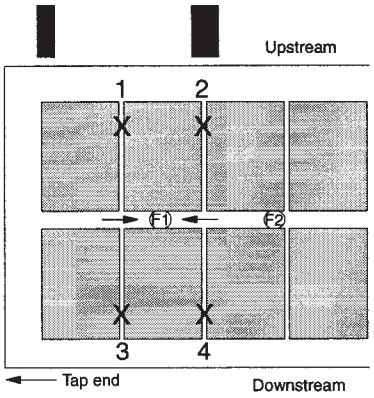

Figure 4 - A section of the cell showing the positions (X) for bath sampling in campaign I when the tracer was added to feeding position F1.

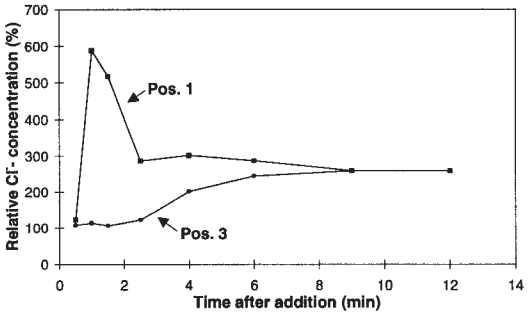

Figure 5 - Relative chloride concentrations measured in positions no 1 and 3 indicated in Fig. 4 as a function of time after addition of 2 kg NaCl in feeding position F1. The chloride concentration is given in percent of the chloride level before addition (approximately 800 ppm. Cl^-).

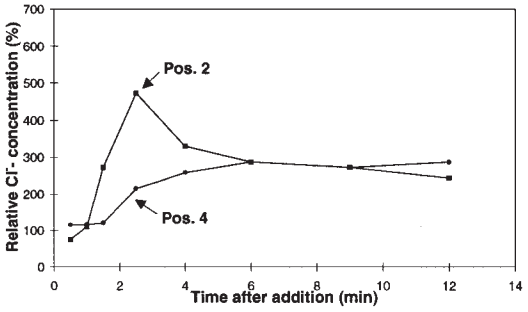

Figure 6 - Relative chloride concentrations measured in positions no 2 and 4 marked in Fig. 4 as a function of time after addition of 2 kg NaCl in feeding position F1.

It is obvious from the curves that the bath flows with higher velocity towards the upstream side of the cell. The time delays between addition and increase in chloride concentration were less in positions 1 and 2 and the increases in chloride concentration were clearly higher in these positions compared to positions 3 and 4. The chloride concentrations on the upstream and downstream sides did not reach the same level until approximately 6-9 minutes after addition of the tracer.

The method of recording the temperature depression was applied for further investigations of the bath flow. Fig. 7 shows the positions where the thermocouples were located in campaign II. The arrows indicate in which regions mean bath velocities could be estimated. The length of the arrows indicates the relative bath velocities. Fig. 8 shows the temperature recorded in a period of 200 s with thermocouples no 1 to 3. The real temperatures shown in this plot do not reflect gradients in bath temperature between the different locations as the temperatures are shifted down by 7 and 12 °C for thermocouples 2 and 3, respectively. This was done so that the responses in each of the positions can be compared more easily.

The mean bath velocities are listed in Table I. These were estimated based on the time delays as explained above.

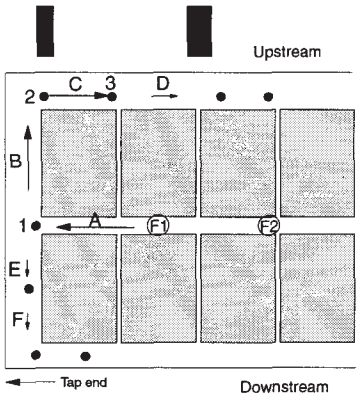

Figure 7 - A section of the cell showing the positions of the thermocouples in campaign II. The regions where mean bath velocities were estimated are indicated by the letters A to F.

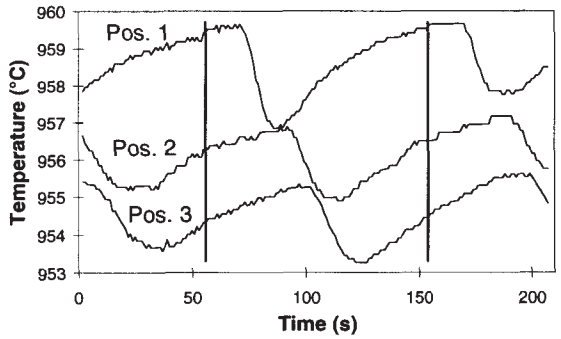

Figure 8 - Recorded temperatures vs time in thermocouples no 1, 2 and 3 as marked in Fig. 7. The absolute temperatures recorded in thermocouples 2 and 3 are shifted down by 7 and 12 °C respectively. The vertical lines indicate the times when alumina batches were added in feeding position F1.

Table I - Calculated bath velocities in the regions shown in Fig. 7 when feeding was made at point F1. The standard deviations indicate the variation in estimated bath velocities from all the alumina batches within one logging period. Table cells marked with "---" indicate no operational thermocouple in that particular run.

	v_{bath} A (cm/s)	v_{bath} B (cm/s)	v_{bath} C (cm/s)	Time after 1. run (h)
Run no 1	9.5 ± 0.5	8.5 ± 1	6.5 ± 2	0
Run no 2	9 ± 1.5	8 ± 0.5	8 ± 2	2-3
	v_{bath} D (cm/s)	v_{bath} E (cm/s)	v_{bath} F (cm/s)	Time after 1. run (h)
Run no 1	- - -	2 ± 0.2	2.5 ± 0.5	0
Run no 2	3 ± 0.5	2 ± 0.2	- - -	2-3

From the temperature responses in thermocouples no 1 to 3 shown in Fig. 8 it is possible to see how the alumina was transported from feeding position F1. The results show that the cooled bath passed towards the end channel, flowed along the end channel towards the upstream side and flowed some distance into the upstream side channel. On the figure only the thermal responses for two of the batches are shown. It can be seen from the standard deviations in Table I that the time delays between addition and temperature drop were very stable throughout the logging period.

The velocity data listed in Table I show that the bath flow rate from the mouth of the centre channel is asymmetric as the velocity is four times higher towards the upstream side. The response from the thermocouple located in the downstream side channel was weaker. Furthermore, the response to the feeding could be recorded at some distance from the short end in the side channel on the upstream side (regions C and D). It is also notable that the bath flow rate dropped to approximately the half in the upstream side channel in the vicinity of the quarter riser (regions C and D).

The asymmetric flow in the end channel was observed in several measuring campaigns. It was therefore demonstrated that this flow pattern was permanent in this type of cell.

In campaign V which was carried out more than two years later, temperature recordings were performed in the upstream region on the same cell. Four thermocouples were located in the upstream side channel and one thermocouple was located in the ACG on the upstream side.

Fig. 9 shows the location of the thermocouples and the regions where the mean bath velocities could be estimated in campaign V. The estimated bath velocities are listed in Table II. Fig. 10 shows plots of temperature vs time recorded in positions 1 and 2 in Fig. 9 for a time period of 200 s.

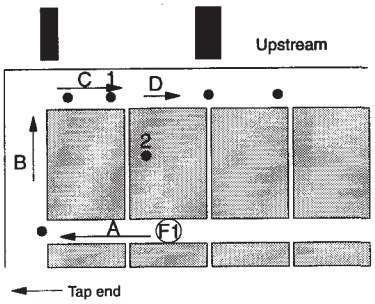

Figure 9 - A section of the upstream side of the cell showing the positions for location of the thermocouples in campaign V. The dark dot on one anode indicates the position for temperature recording in the ACG.

Table II - Calculated bath velocities in the regions shown in Fig. 9 when feeding was made at point F1.

v_{bath} A (cm/s)	v_{bath} B (cm/s)	v_{bath} C (cm/s)	v_{bath} D (cm/s)
6.8 ± 0.3	5.0 ± 0.3	5.0 ± 0.7	2.8 ± 0.4

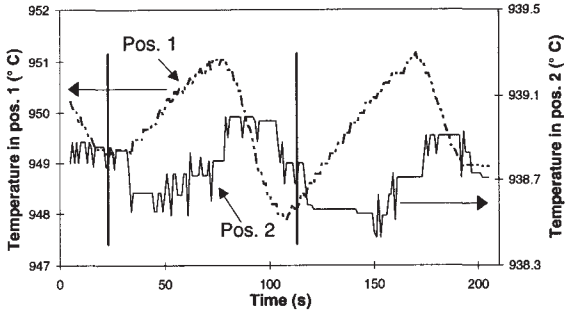

Figure 10 - Temperatures vs time recorded with thermocouples no 1 and 2 marked in Fig. 9. The vertical lines indicate the times when alumina batches were added in the feeding position F1.

The results from campaign V also showed that the bath flow rate in the upstream side channel decreased by almost one half in the region where the quarter riser is located (regions C and D in Fig. 9). By comparing the temperature responses in positions 1 and 2 one can see that some of the cooled bath was transferred down to the ACG after it had passed the thermocouple in position 1. The time difference between the responses in positions 1 and 2 was approximately 25 s.

The fact that the recorded temperature in the thermocouple located in the ACG was approximately 10 °C lower than the temperature measured in the side channel is probably due to the cooling effect from the newly set anode.

Alumina transferred from an inner feeder

In campaign I tracer was added in feeding position F2 and bath sampling was performed in two locations. Fig. 11 shows where the bath samples were collected, and the relative chloride concentrations versus time after addition are plotted in Fig. 12.

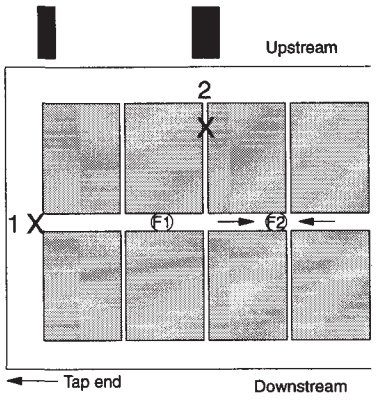

Figure 11 - A section of the cell showing the positions (X) for bath sampling in campaign I when the tracer was added to feeding position F2.

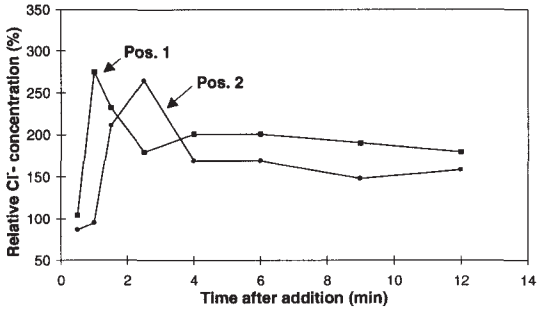

Figure 12 - Relative chloride concentrations measured in positions no 1 and 2 indicated in Fig. 11 as a function of time after addition of 2 kg NaCl in feeding position F2.

It is seen from Fig. 12 that the tracer added to feeding position F2 was transferred the same way as was the tracer added in position F1. By comparison with Fig. 6 it is seen that the increase in chloride concentration was less when tracer was added to the inner feeder location, which must be attributed to the higher degree of dilution of the tracer in the latter case.

By comparing the responses in position 2 in Figs. 6 and 12 it can be seen that the time delays between addition and increase in chloride concentration were the same for addition to positions F1 and F2. However, comparison of absolute bath velocities can be misleading in this case. Firstly, the uncertainty in the time delay is high for these measurements since bath sampling was done at time intervals of 30 seconds. Secondly, these two measurements were made on two different cells.

Fig. 13 shows the locations of the thermocouples when the alumina transport from an inner feeder was studied. Measurements of this kind were performed in two measuring campaigns on the same cell with a time interval of 13 months. In the figure circles and quadrangles represent the locations of the thermocouples in campaigns III and IV respectively. A circle inside a quadrangle means that a thermocouple was positioned in this location in both campaigns. In Table III the time delays from feeding to initiation of temperature drop in campaign III are listed, while in Table IV the estimated bath velocities from the measurements in campaign IV are given.

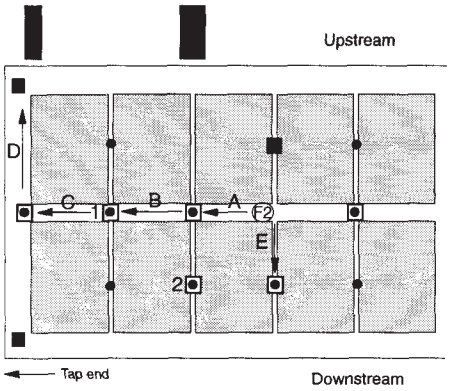

Figure 13 - A section of the cell showing the positions for location of the thermocouples in campaigns III (•) and IV (■).

Table III - Calculated time delays in the points shown in Figure 13 when feeding was made at point F2 in campaign III.

Time delay point 1 (s)	Time delay point 2 (s)
45 ± 9	37 ± 7

Table IV - Calculated bath velocities in the regions shown in Fig. 13 when feeding was made at point F2 in campaign IV.

	v_{bath} A (cm/s)	v_{bath} B (cm/s)	v_{bath} C (cm/s)	Time after 1. run (h)
Run no 1	6.5 ± 1.4	3.8 ± 0.7		0
Run no 2	9	8.5	5	1/2
	v_{bath} D (cm/s)	v_{bath} E (cm/s)		Time after 1. run (h)
Run no 1		3.4 ± 0.3		0
Run no 2	7	8 ± 5 *		1/2

* The velocity in this direction decreased from 14 to 4 cm/s within 18 minutes.

In campaign III responses to feeding from point F2 were rare. In only two of the thermocouples some slight temperature drops were recorded. It is also notable that while a weak response to the alumina batches was recorded in point 1 on Figure 13 ($\Delta T < 0.5$ °C), no response was detected in the thermocouple located between feeder F2 and thermocouple no 1. This observation could indicate that the alumina was transferred directly from point F2 down into the ACG and from there in the direction of the end channel.

In the first run in campaign IV clear responses to all batches were recorded, which made it possible to estimate bath velocities in regions A, B and E. In the second run, however, only the first of altogether five batches was recorded in the thermocouples located within the directions A, B, C and D. In this case no standard deviations could therefore be calculated for the bath velocities. In region E three of the batches were recorded in the second run. The time delay between feeding and response in this direction increased significantly within the logging period, corresponding to bath velocities of 14 and 4 cm/s for the first and last batches respectively.

The results from the three campaigns where alumina transport from the inner feeder were studied, showed that the bath flow in the vicinity of the inner feeder is highly unstable. In some cases the added tracer or alumina was clearly recorded in the same regions as tracer and alumina were detected when added to point F1. In other cases, as in campaign III and in the main part of the second run in campaign IV, the effect of the batches was hardly detectable. The batches that were detected in these cases were recorded as weak signals, i.e. the temperature drops were small. Furthermore, responses to feeding were never recorded in the small gaps traverse to the centre channel on the upstream side of the cell.

Measurement of anode gas release

The amount of gas released from the short sides was measured on both sides of two anodes. Anode gas was collected at several positions on the short side as shown in Fig. 14. Some part of the anode sides facing the centre channel could not be reached with the equipment used because access was blocked by feeder and silo.

Figs. 15 and 16 show bar charts of the measured anode gas release per minute in the different positions.

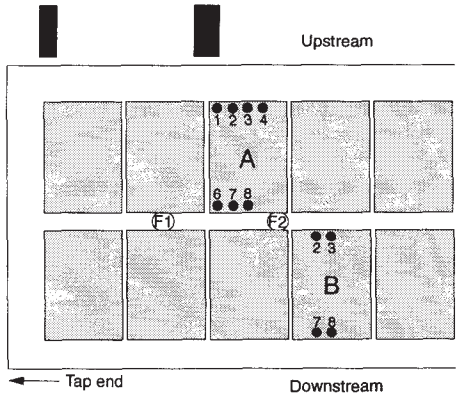

Figure 14 - A section of the cell showing the positions for collection of gas released from the anode. Each position represents 15 cm of the anode side.

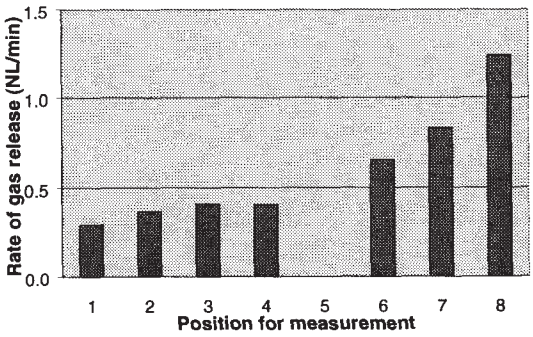

Figure 15 - Rate of gas release from anode A in the locations shown in Fig. 14.

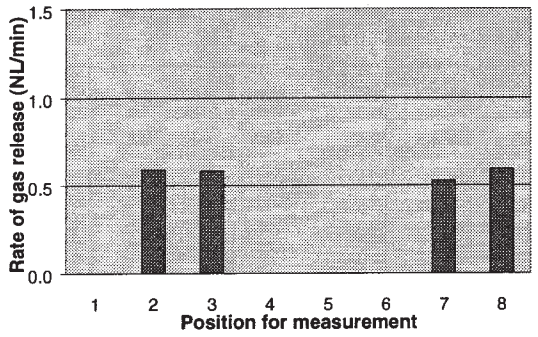

Figure 16 - Rate of gas release from anode B in the locations shown on Fig. 14.

The rates of gas release from both anodes were higher in the middle of the short sides (positions 2-4 and positions 7-8). This difference would be expected if the anode gas takes the shortest way to the edge. However, the amount of gas collected was in average only about 45% of that estimated when considering "shortest way of travel" for the gas. The most probable explanation is that the funnel did not collect all the gas.

The most striking result from these measurements is the uneven distribution of anode gas from anode A. The rate of gas distribution into the centre channel was 2-3 times higher than the rate of gas release into the side channel from this anode. No such effect was seen on anode B.

Discussion

Both the tracer measurements and the measurements of the temperature depression in the bath after alumina addition showed that for this type of cell the alumina is transferred preferentially to the upstream side. This finding is consistent with the fact that the frequency of formation of spikes and deformations is clearly lower for the anodes on the upstream side of this cell. It was also shown that the alumina is transferred via the end channel when added to an outer feeder.

Measurements with tracer additions gave only a rough picture of the flow situation. The temperature measurements made it possible to investigate more thoroughly the bath flow in the centre, end and upstream side channel in the regions near the outer feeder. It was seen in several campaigns that the bath velocity in the end channel from the mouth of the centre channel towards the upstream side is 2.5 - 4 times higher than towards the downstream side. Bath velocities of the same magnitude were measured in the following three regions: (i) the centre channel between the outer feeder and the end channel, (ii) the half of the end channel between the mouth of the centre channel and the upstream side and (iii) the upstream side channel between the end channel and the first anode gap (regions A, B and C respectively in Figs. 7 and 9, see Tables I and II). In the region between the first and second anode gap a marked reduction in the bath velocity was observed (region D in Figs. 7 and 9) compared to bath velocities in the above mentioned regions. In the ACG between the first and second anode gap it was recorded a temperature response approximately 25 seconds after the temperature drop was recorded in the thermocouple located near the first anode gap in the upstream side channel (pos. 1 and 2 in Fig. 9). Thus it can be concluded that the bath is transferred into the ACG from the side channel. The observation of reduced bath velocity on the upstream side indicates that there is an increase in the amount of bath entering the ACG from the upstream side channel somewhere between the first and second anode gaps.

The vertical, downward electric current through the anode rods and the anode blocks gives rise to the main horizontal magnetic field in the cell. This field decreases from the outer part towards the centre of the cell. When this field interferes with the vertical current in the bath, it creates Laplace forces pointing from the outer parts towards the middle of the cell. On side-by-side cells where the current is conducted to the anode bus system by quarter risers located at the upstream side, the magnetic field and thus the force field in the ACG is amplified on the upstream side near the risers. This situation causes an asymmetry in the force field between the upstream and downstream sides. It has been shown in a MHD model made by Hydro Aluminium that in the regions where this asymmetry in the force field is present the bath velocity is higher in the ACG on the upstream side compared to the velocity on the downstream side. Fig. 17 shows estimated bath velocities in the cell used in the present study by applying this model. The maximum and minimum bath velocities in these calculations are 15 and 0.2 cm/s, respectively, while the mean velocity is 4.5 cm/s.

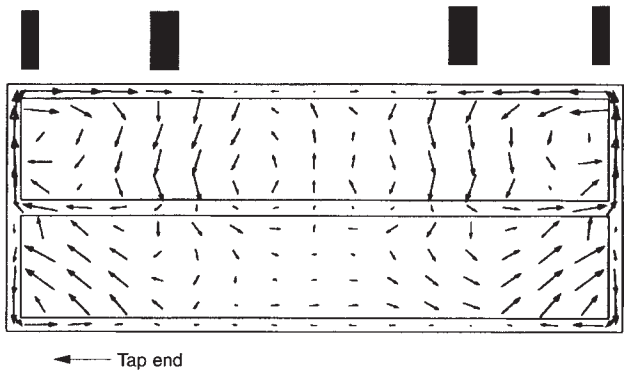

Figure 17 - Bath velocities in the cell used in the present study calculated in a MHD model made by Hydro Aluminium. The vectors drawn on the positions of the anodes show the calculated velocities midway between the bath/metal interface and the working surface of the anodes, while the vectors drawn in the channels show the calculated velocities midway between the bath/metal interface and the bath surface.

Both the experimental results and the MHD-calculated bath velocities shown in Fig. 17 give a picture of a bath flow bounded lengthways by the centre channel and the upstream side channel and bounded crosswise by the end channels and the quarter risers. Such a flow situation would imply that the bath under the anodes no 2 and 3 counted from the end channels on the upstream side should have a good supply of alumina. This is consistent with the fact that these anodes are practically immune to the spike and deformation problems described in the "Introduction" chapter (see Fig. 2). The dissolution of alumina in this region should be rapid since the alumina meets a high proportion of "fresh" bath which is beneficial for heat and mass transfer. The bath should therefore be charged with a high content of *dissolved* alumina when it enters the region under these anodes.

The measurement of gas release showed clearly that the gas release into the centre channel was dependent upon location. The choice of anodes A and B on Fig. 14 for these measurements was made on basis of the MHD model saying that the bath flow under these anodes was

particularly high and low respectively. It can be concluded on the basis of the results that the bath flow set up by the MHD forces is able to drag the gas bubbles in the direction of the flow. It can therefore be assumed that when escaping towards the bath surface the gas bubbles drag the bath from the ACG up into the region above the working surface. This implies that there should be a high rate of bath flow into the centre channel which sets up the circulating, horizontal bath flow described above.

The implication for the middle part of the cell is that the bath flow rates into the centre and side channels do not differ significantly. There will therefore be a more stationary flow situation towards the mid-section of the cell with less horizontal transport of bath. Alumina added into the mid-region of the centre channel will thus not be carried away effectively from the feeding position.

The fact that the inner feeders were located at the "border" between the non-stationary and the stationary regions in the centre channel can explain why clear thermal responses on batches added from these feeders only periodically were recorded.

One can only speculate what happens with the alumina in those periods where the batches added to the inner feeders are not carried away by the circulating bath flow. Probably, the alumina stays floating on the bath surface in the vicinity of the feeder for some time until the bath has penetrated the alumina. After sinking the alumina agglomerates can be transferred into the ACG. In Fig. 17 it can be seen that the MHD-calculation proposes a weak bath flow in the ACG in this region from the centre towards the downstream side. This is consistent with the experimental results, since responses in the thermocouples located in the small traverse gaps were only recorded on the downstream side.

In the latter case the conditions for alumina dissolution should be less beneficial since the alumina meets little "fresh" bath when not being transferred quickly away from the feeding location. Accordingly one might expect that there would be more build-up of muck in the cell in periods with this kind of feeding situation.

Acknowledgements

The authors gratefully acknowledge financial support from the Research Council of Norway and from the Norwegian aluminium industry. They are also indebted to Henrik Gudbrandsen, Trygve Ringstad, Sverre Rolseth and Jomar Thonstad for participating in practical and theoretical parts of the work. Thanks should also be given to personnel at the Hydro Aluminium plants in Årdal and Karmøy as well as to personnel at the research centres in Porsgrunn and Årdal.

References

1. E. Dernedde, E. L. Cambridge. "Gas Induced Circulation in an Aluminium Reduction Cell". Light Metals 1975, pp. 111-132.

2. A. Solheim, S.T. Johansen, S. Rolseth, J. Thonstad. "Gas Driven Flow in Hall-Heroult Cells". Light Metals 1989, pp. 245-252.

3. D. C. Chesonis, A. F. LaCamera. "The Influence of Gas-Driven Circulation on Alumina Distribution and Interface Motion in a Hall-Heroult Cell". Light Metals 1990, pp. 211-220.

4. J. M. Purdie, M. Bilek, M. P. Taylor, W. D. Zhang, B. J. Welch, J. J. J. Chen. "Impact of Anode Gas Evolution on Electrolyte Flow and Mixing in Aluminium Electrowinning Cells". Light Metals 1993, pp. 355-360.

5. M. L. Walker, J. M. Purdie, N. S. Wai-Poi, B. J. Welch, J. J. J. Chen. "Design Consideration for Selecting the Number of Point Feeders in Modern Reduction Cells". Light Metals 1995, pp. 363-370.

6. J.J.J. Chen, X. Shen, M. P. Taylor, B. J. Welch. "A Study of Bath Distribution in a 3-D Water Model". Light Metals 1996, pp. 343-350.

7. R. Shekar, J. W. Evans. "Physical Modeling Studies of Electrolyte Flow due to Gas Evolution and Some Aspects of Bubble Behavior in Advanced Hall Cells: Part I. Flow in Cells with a Flat Anode".Met. Trans. B, **25B**, pp. 333-340.

8. J. W. Evans, S. K. Banerjee. "A Physical Model for Melt Flow in Hall Cells". Light Metals 1986, pp. 535-539.

9. S. D. Lympany, D. P. Ziegler, J. W. Evans. "The Hall-Héroult cell: some Design Alternatives examined by a Mathematical Model". Light Metals 1983, pp. 507-517.

10. W. E. Wahnsiedler. "Hydrodynamic Modeling of Commercial Hall-Heroult Cells". Light Metals 1987, pp. 269-287.

11. M. Segatz, D. Vogelsang, C. Droste, P. Baekler. "Modelling of Transient Magneto-Hydrodynamic Phenomena in Hall-Héroult Cells". Light Metals 1993, pp. 361-368.

12. M. M. Bilek, W. D. Zhang, F. J. Stevens. "Modelling of Electrolyte Flow and its Related Transport Processes in Aluminium Reduction Cells". Light Metals 1994, pp. 323-331.

13. K. Grjotheim, C. Krohn, R. Næumann, K. Tørklep. "On the Application of Radiotracers in the Aluminium Industri". Light Metals 1971, pp. 133-145.